Oceanological and Hydrobiological Studies

International Journal of Oceanography and Hydrobiology

Volume 45, Issue 1, March 2016
pages (20-34)

ISSN 1730-413X
eISSN 1897-3191

Groins and submerged breakwaters – new modeling and empirical experience[a]

by

Rafał Ostrowski*, Zbigniew Pruszak, Jan Schönhofer, Marek Szmytkiewicz

DOI: **10.1515/ohs-2016-0003**
Category: **Original research paper**
Received: **April 30, 2015**
Accepted: **July 22, 2015**

Institute of Hydro-Engineering of the Polish Academy of Sciences, ul. Kościerska 7, 80-328 Gdańsk, Poland

Abstract

The relationship between the effectiveness of groins and their technical condition was studied. The supporting role of groins in artificial shore nourishment was tested using the theoretical modeling of hydrodynamic and morphodynamic processes in the nearshore zone. This modeling scheme was developed as to represent the actual coastal situation occurring on the shores of the Hel Peninsula (the Gulf of Gdańsk, the southern Baltic Sea). Based on the results of computations and the results of field observations, recommendations were prepared on the design and maintenance of groins. The second part of the paper is devoted to submerged breakwaters. The theoretical modeling of wave-current fields near the segmented submerged breakwaters led to the determination of coefficients of wave transmission and rip current velocities, which finally yielded a piece of design advice. In all numerical simulations, the Delft3D software was used.

Key words: groins, submerged breakwaters, interaction with artificial shore nourishment, rip currents

* Corresponding author: *rafal.o@ibwpan.gda.pl*

[a] Paper presented at the PROZA Conference "*Modelling of hydrodynamic phenomena in the Baltic Sea — PROZA project in view of modern research*", Gdynia, Poland, 16th October 2012. The project PROZA, entitled „*Operational decision-making based on atmospheric conditions*" is a part of the Polish Innovative Economy Programme.

DE GRUYTER

The *Oceanological and Hydrobiological Studies* is online at oandhs.ocean.ug.edu.pl

Introduction

The coastal zone is subject to continuous evolution due to the influence of waves and currents. Recently, coastal changes hae become increasingly intensive. As a result, many seashores, mostly the sandy ones, are gradually but permanently retreating. As coastal regions are densely populated and additionally attractive for tourists in the summer season, the shore protection against erosion and flooding is necessary. The protection activities are preceded by decisions on technical measures to be applied. In the previous decades, revetments and groins were the most popular coastal protection structures (Pilarczyk & Zeidler 1996; Kunz 1996). Groins, especially in the form of timber palisades, are relatively cheap and easy to build, but their effectiveness largely depends on the technical condition, as well as local environmental factors, mostly parameters of hydrodynamic and lithodynamic processes. In particular, the coastal sea bed profile together with the nearshore resources of sandy sediments and the resulting morphodynamic processes play an important role. The supply of sandy material can be natural (longshore sediment transport) or artificial (shore nourishment). Thus, the meaning and efficiency of groins strictly depend on both the availability of appropriate sand and structural issues. According to Aminti et al. (2004), the groin tip should reach the first underwater bar, particularly if the shore is artificially nourished. Such a length of groins is favorable to recovery of the natural nearshore sea bed profile, improves the shore stability, prolongs the nourishment duration and raises the effectiveness of the groin system. It should be pointed out that many of the currently occurring groin systems were built a long time ago and therefore, the technical condition of some groins is inferior, presumably causing their lesser effectiveness.

Nowadays, there is a clear preference to implement the shore protection methods which are environmentally friendly and invisible to tourists, whenever possible. These criteria can be met by applying the artificial shore nourishment or construction of submerged breakwaters.

In case of intensive erosion and significant deficit of sediments, the artificial shore nourishment is most effective. It can be applied as the sole shore protection measure or as a supplementary method, supporting the existence of "hard" engineering defense in the form of groins, breakwaters or revetments. Similarly to the other means of shore protection, the artificial nourishment is accompanied by a number of problems and constraints related, for instance, to the availability of sediment borrow areas with sand of appropriate quality. In addition, ecologists claim that interventions in the sea bottom, associated both with dredging and beach fills, are harmful to the benthic ecosystem. Therefore, it is recommended to carry out artificial nourishment operations rarely enough to let the environment recover after a disturbance. Thus, it appears necessary to prolong the duration of nourishment. In view of the above, it seems sensible to implement combinations of artificial shore nourishment and coastal structures which can increase the period between re-nourishments. The submerged breakwaters and groins can be such structures which positively interact with the artificial nourishment and help to retain sandy material in the nearshore area.

Recently, coastal engineers are more and more often faced with a problem of damaged and malfunctioning groins. Is it viable to renovate the old groins or to build the new ones on the shore with the nourishment carried out? What should submerged breakwaters be like, either separate structures or interacting with nourishment, in order to optimize the sediment management and minimize the side effects, e.g. rip currents? The present paper is an attempt to answer these questions.

Materials and methods

The objectives of the study are based on the theoretical modeling and field observations, as well as the analysis of information available in literature.

The theoretical (numerical) modeling of hydrodynamic and morphodynamic processes around complete and damaged groins was carried out using the Delft3D software (Deltares 2010a, 2010b). The Delft3D is a multi-dimensional (2D or 3D) hydrodynamic (and transport) simulation program which calculates a non-steady flow and transport phenomena resulting from tidal and meteorological forcing on a curvilinear, boundary-fitted grid or spherical coordinates. Both currents and waves act as driving forces, and a wide variety of transport formulae were incorporated. Wave simulation is carried out using the phase-averaged model (SWAN), including wave breaking and wave-current interaction. Sediment transport rates are determined on the basis of parameters of waves and wave-driven currents. The Delft3D model has already been used at IBW PAN, recently calibrated and validated in relation to the wave-current laboratory and field data

(Schönhofer 2014), which comprise rip currents, both on the natural shore and induced by submerged breakwaters. The calibration activities have yielded the main finding that the wave transformation model can be well tuned by the wave breaking coefficient while the patterns of wave-driven currents mostly depend on friction factors, and in a smaller degree – on eddy viscosity. During the present study, based on the above-mentioned calibrations and sensitivity analysis, the following crucial model parameters were defined: the wave breaking coefficient $\gamma = 0.7$, bottom roughness expressed by Chézy's coefficient $C = 45\ m^{0.5}\ s^{-1}$ and eddy viscosity $\nu = 1\ m^2\ s^{-1}$.

For the purpose of computations concerning groins, it was assumed that the initial bathymetric system was uniform along the shore, according to one of the typical multi-bar cross-shore profiles measured on the Hel Peninsula in 2010; see Fig. 1, for the location of the study site. Bathymetric conditions of the Hel Peninsula are characterized by a gentle inclination of the nearshore sea bottom, namely from 1% to 2%. Such a shore hardly reflects waves, and the wave transformation process is dominated by wave energy dissipation, mainly due to wave breaking. The nearshore sea bed is built of fine sand, having $d_{50} \approx 0.2$ mm. Aside from the groins, the safe maintenance of the Hel Peninsula coast is provided by artificial beach nourishment on the shore segments stretching 23.5 km south-eastward from the base of the peninsula. Reconstruction of the long-term local wave climate shows that during the extreme storm with the return period of 10 years the significant offshore wave height is H_s=6.27 m and the wave energy peak period is T_p=12 s. The respective wave parameters for 1-year storm conditions are H_s = 3.13 m and T_p = 8 s. According to various estimations, the net longshore sediment transport rate amounts to 100 000 – 200 000 $m^3\ year^{-1}$.

Figure 1

Location of the Hel Peninsula in the Baltic Sea

In the successive model tests, the middle groin of the three-groin system was assumed to be complete or damaged in various ways. The modeling has provided current fields for all the considered situations.

In the modeling of the artificial nourishment duration, it was assumed that the artificial nourishment was applied to the above sea bed in the nearshore zone between the shoreline and the first bar. The computations were carried out for the entire multi-bar cross-shore profile occurring at the Hel Peninsula. The modeling of the nearshore region within the finest grid (including the first bar) is shown in Fig. 2. The sandy material filled two fields between three complete, undamaged neighboring groins. The computations have yielded parameters of waves and currents in the fields between the groins.

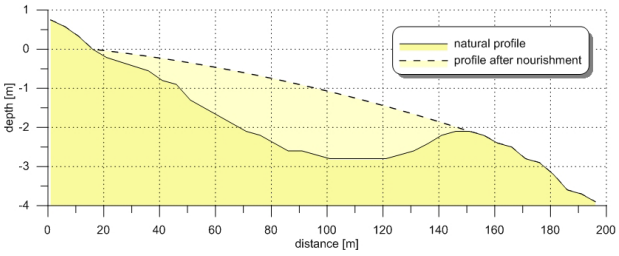

Figure 2

The nearshore part of the cross-shore profile at the Hel Peninsula

Field observations focused on the groin system located on the Hel Peninsula and stretching 8 km along the open sea side from the Peninsula's base. The survey was carried out in June 2011 and covered the location of the groins with respect to the shoreline, accumulative and erosive effects, technical condition of the groins and their lengths.

The issue of submerged breakwaters was dealt with by the theoretical modeling only, also using the Delft3D computational package. In the modeling focused on wave and current fields, a constant sea bottom inclination of 0.02 was assumed to represent a typical south Baltic nearshore area. The height of breakwaters and gaps between them were changed in the consecutive model runs while the crest width of breakwaters (in the cross-shore direction) was kept constant. To investigate the influence of the crest width, a phase-resolving model would be more suitable. Thus, the present study focuses on the large-scale geometrical parameters of the submerged

breakwaters. The results are presented mostly in the dimensionless form, as functions of the ratios of the water depth at the breakwater crest to the water depth and the breakwater segment length to a gap between segments.

Groins

Experience on mechanisms of groin-shore interaction

Usefulness of groins on a considered coastal segment depends on the local wave climate and sediment resources, as well as anticipated variability of these factors. The state-of-the-art experience on groins indicates the following:

- groins are recommended on the shores where sediments are available in a satisfactory quantity, either naturally or via artificial nourishment;
- the resultant wave energy flux is quantitatively large and directed obliquely to the shore;
- if the sediment supply is sufficient, groins cause beach accretion, particularly during the first years after the construction, and maintain the accumulated shore for a long time;
- on the shores suffering from lack of sediments, groins accumulate a narrow and low beach, not resilient to waves during storm surges, which often cause the dune erosion.

General rules of interactions between the shoreline, sediments and groins have been investigated for many decades, also recently (Badiei et al. 1994; Hanson et al. 1996; Kunz 1996; Bacamo & Grosskopf 1999; Dabess et al. 2004; Nakamura 2010). It can therefore be expected that the basic recommendations on planning and design of groins are well known and reliable.

The experience concerning groins shows, however, that they can affect the seashore (under similar bathymetric and hydrodynamic conditions) either favorably or adversely. Recent studies have made efforts aimed at better understanding of groins – shore interaction and further improvement of the design guidelines.

Studies devoted to the assessment of groins' impact on a multi-bar seashore have led to the conclusion that the functionality of a groin increases as long as it actively works together with a system of the nearshore morphology (Fleming 1991). This is particularly important to an artificially nourished shore. Conservation or restoration of the natural cross-shore profile with large bed forms considerably improves the coastal stability, increases the durability of artificial nourishment and raises the effectiveness of groins. The above has been deduced from the theoretical considerations and numerical modeling, as well as field surveys carried out on multi-bar seashores (Pruszak et al. 2000; Pruszak 2004).

It should be noted that bars, both natural and restored by nourishment, aside from playing a role of sediment stocks, are a reason for wave energy dissipation at a distance from the shoreline. Analysis of the south Baltic data shows (Raudkivi & Dette 2002) that the nourishment operation is more successful and permanent if the supplied sandy material creates across-shore transect shape close to the so-called equilibrium profile, conducive to the gradual wave energy dissipation. A steep cross-shore profile, either natural or with groins, is usually less stable and displays erosive tendencies.

Long-term German observations of groins' effectiveness, carried out on the East Frisian Islands (including Norderney) since about 1900, have shown that groins themselves prove to be totally inefficient in this region (Kunz 1996). Erosion of beaches and dunes was stopped only when the artificial shore nourishment was implemented. As evidenced by field investigations, groins play a very important role, supporting the nourishment through accretion of the shore. This has inspired the German Federal State of Lower Saxony to renovate and restore some of the groins in the region. Groins have not been, however, recommended as the sole shore protection measure in the case of long-term persistent coastal erosion.

Suggestions on the structural improvement of groins concern the optimization of both dimensions of single groins and geometries of the entire groin systems (Trampenau et al. 1996; Hanson et al. 2010; Nakamura 2010; Uno et al. 2010). The length of a groin is one of the most important dimensions. Longer groins cause more intensive accumulation of sand but result in much more serious lee-side erosion. This lee-side effect is not that harmful for shorter groins which, however, trap smaller fractions of the longshore sediment flux.

According to Nakamura (2010), if the water depth at a groin tip h_k is equal to the significant wave height $H_{\hat{s}}$ corresponding to the long-term mean energy of waves reaching the shore vicinity, about 40% of the longshore sediment transport is trapped

within the groin system. An increase in the depth h_k results in the increased accumulation capacity and will yield almost 100% for $h_k/H_s \approx 3$. For the Polish (south Baltic) coast, with the typical mean stormy value of $H_s \approx 0.9$-1.0 m, assuming $h_k \approx 2.0$-2.5 m, one can expect that about 70% of the longshore sediment flux will be accumulated by the groin system.

As indicated by the observations, the optimization of the permeability of groins can be crucial for their effectiveness. The permeable groin is intended to slow down the longshore flow of water and sediments, instead of blocking it completely. Ultimately, the permeability of the whole groin system will induce both accumulation of sand between the groins and the lee-side erosion. As proposed by Trampenau et al.(1996), the gradually increasing permeability of a groin along its length from a root to a tip results in a less violent disturbance of longshore sediment transport. Most studies suggest that the best results are provided by groins having the permeability of about 30%. In the region of Warnemünde, high effectiveness was achieved by groins with the permeability of 50% (Trampenau et al. 1996). In addition, permeability of groins contributes to the reduction of wave run-up effects and velocities of the cross-shore currents, like return flows and rip currents, which would be amplified by impermeable groins.

The results of field observations carried out worldwide imply that for specific coastal geometries, the intensification of accumulative effects can be achieved through an elongation of groins and an increase in the longshore spans between them. This results in a more distinct wave diffraction around groins' tips, which in turn leads to the reduction of longshore current velocities and longshore sediment transport rates. This phenomenon is typically observed in regions of the bay-type shores (Schoonees et al. 2006).

Field experiments and the related numerical simulations carried out in the USA by CERC (Coastal Engineering Research Center) have revealed that a considerable slowdown in the lee-side erosion can be obtained by reducing the length of the last groins in the system (Hanson et al. 2010). This solution is a compromise because smaller accumulation can be expected within the groins located at the end of the system but the lee-side effect beyond the system is partly mitigated. In the case of artificial nourishment applied as a supplementary shore protection measure, the shortening of the last groins in the system can increase the nourishment efficiency and prolong the re-nourishment timespan by about 20-25%.

Analysis of interactions between the seashore and damaged groins

As mentioned before, it is believed that the usefulness of groins largely depends on their technical condition. Timber pile groins (most popular on the southern Baltic coast), begin to malfunction after a few decades due to more or less serious damage. In the Baltic conditions, the vulnerability of coastal structures to destruction increases in the winter season when ice phenomena (bringing additional loads on structures) overlap with stormy hydrodynamic impacts. Timber palisades are exposed to decay in water, the results of which is visible after about 15 years. This corrosion leads to the reduction of diameters of piles, as well as their resistance to breaking and washing out from the sea bed. A lack of single piles in the groin structure does not have a significant influence on the groin effectiveness as it only locally increases its permeability, while a breach comprising a few piles results in an increase of current velocities in the structure segment where piles are missing. This causes scouring and decreases the accumulation capacity of the groin.

A question arises what should be done with a malfunctioning groin or a groin system on the shore segment where artificial nourishment is carried out or planned. An answer was sought using numerical modeling by the Delft3D software for the cases of damaged groins (breach constituting 1/3 of the groin length) and a groin in good technical condition, as well as the natural seashore.

The following cases were considered:

- no groins;
- groins in good condition;
- missing piles in the root part of the groin;
- missing piles in the central part of the groin;
- missing piles at the groin end.

In all the above cases, nearshore current velocities are of the utmost importance. The computational layout was based on the actual system of timber palisade groins stretching along the Hel Peninsula shore (the Gulf of Gdańsk, the southern Baltic). The groins were built in the period from 1946 to 1961 and are now in various technical condition, from good to heavily damaged. The modeling area stretched 500 m in the longshore direction and 1200 m in the cross-shore direction. Bearing in mind the structural features and permeability of the groins (palisades with narrow gaps between the piles), values of both the reflection coefficient and the transmission

coefficient were assumed to be equal to 0.5. The other conditions were assumed as follows:

- groins' length equal to 60 m (counted seaward from the shoreline);
- span between neighboring groins equal to 90 m.

Numerical modeling of nearshore wave-driven currents was carried out for typical conditions of frequently occurring mild storms in the south Baltic coastal zone (Pruszak et al. 2000). The respective parameters were as follows: significant wave height H_s=1 m, wave energy peak period T_p=4 s and wave to shoreline angle a=45°. These parameters were assumed at the offshore location, namely 1000 m from the shoreline. The nearshore computational grid (in the zone of 0-200 m from the shoreline) had the dimension of 5 m, while the computational grid in the outer zone (200-1200 m from the shoreline) had the dimension of 15 m.

Computational results

Natural shore (no groins)

A typical pattern of the longshore wave-driven flow has been obtained for the natural shore, with the characteristic zones of velocity ranges (Fig. 3). Velocities of 0.4-0.5 m s^{-1} were obtained for a strip of about 10 m width, located in the close vicinity of the shoreline. The next zone, 50 m wide, shows velocities of 0.2-0.4 m s^{-1}, while the outer zone, 60 m wide, has velocities of 0.1-0.2 m s^{-1}. For the sediments typically occurring on the shores of the Hel Peninsula, characterized by the median grain diameter d_{50}=0.15-0.25 mm, the incipient sea bed grain motion starts when the flow velocity amounts to 0.1 m s^{-1}, while the bulk sediment transport is driven by flow velocities of 0.2-0.4 m s^{-1}. For practical engineering purposes, it has been assumed that the critical flow velocity, causing a relatively intensive motion of sea bed grains, equals to 0.2 m s^{-1} for the considered sand. The obtained modeling results evidence that the considered hydrodynamic conditions induce the sediment motion in the zone stretching 60 m seaward from the shoreline and that this motion is intensive in the nearshore region, up to 10 m from the shoreline.

Groins in good condition (full length groins)

The presence of the groin system significantly reduces the flow velocities (Fig. 4). The maximum velocities (0.1-0.2 m s^{-1}) occur not farther from the shoreline than about half the groin length. Beyond this line, the flow velocities do not exceed 0.1 m s^{-1}, while beyond the groins tips the values are in the range 0.05-0.1 m s^{-1}, thus also smaller than their counterparts for the natural shore. The effect of groins is not visible at a distance larger than 80-90 m from the shoreline where the velocities are the same as in the case of the natural shore (Fig. 3). In the considered wave conditions, the presence of groins considerably reduces the velocities of the nearshore currents and the rates of sediment transport induced by these currents.

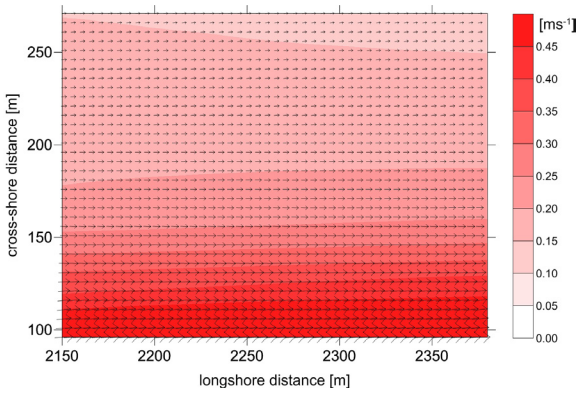

Figure 3

Calculated depth-averaged flow velocities for the natural nearshore zone (without groins) in moderate storm conditions (H_s=1 m, T_p=4 s, α=45°)

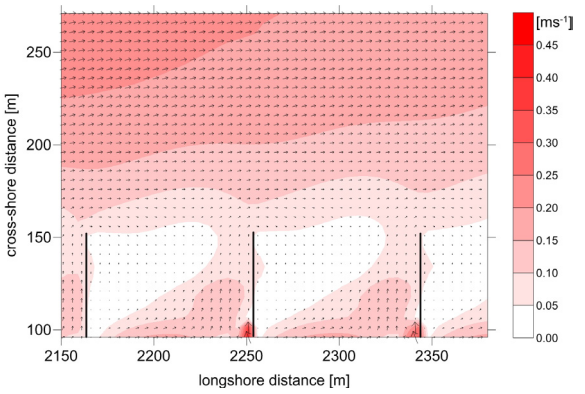

Figure 4

Calculated depth-averaged flow velocities for full length groins in moderate storm conditions (H_s=1 m, T_p=4 s, a=45°)

Groin with a breach at its root (missing 1/3 of the groin length at the shoreline)

In this case, one groin in a system displays a lack of piles in 1/3 of the groin length at the shoreline (no contact of the groin with land), while the other groins in the system are undamaged (Fig. 5). A strong current is visible in the breach (between the shoreline and the structure), having velocities of 0.2-0.4 m s^{-1}. This current is also present far rightward on the lee side of the malfunctioning groin, obviously causing the sea bed erosion close to the shoreline. The flow pattern depicted in Fig. 5 indicates that the sediment mobilized in this way will be transported and moved in the seaward direction along the neighboring groin.

Further, it can be seen in Fig. 5 that one malfunctioning groin in the system can be more harmful to the shore than the total lack of groins (cf. Fig. 3). In the case when a groin is separated from the shoreline, the sediment is transported from the shoreline vicinity to remote offshore locations while in the situation when there are "no groins", the sediment is transported along the shoreline.

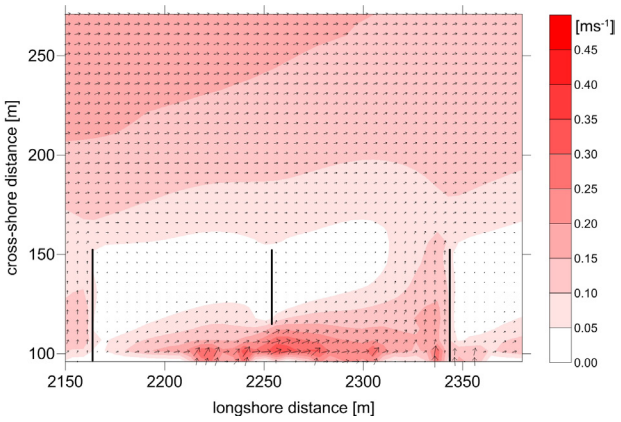

Figure 5

Calculated depth-averaged flow velocities for a groin separated from the shoreline in moderate storm conditions (H_s=1 m, T_p=4 s, α=45°)

Groin with a breach in its main body (missing 1/3 of the groin length in its central part)

This situation is similar to the previously analyzed situation, a breach in the groin brings about similar local intensification of a flow at the location of the damage (Fig. 6) but the velocities are not that high (cf. Fig. 5), i.e. 0.2-0.4 m in the close vicinity of the breach only. In the remaining region, adjacent to the shoreline, the velocities are equal to 0.1-0.2 m s^{-1}.

Sediment originating from the sea bed erosion at the groin breach will be transported to the lee side and next in the cross-shore direction, seaward along the neighboring "healthy" groin (Fig. 6). This process, however, will be less intensive than in the case of the groin with the breach at the structure root (cf. Fig. 5).

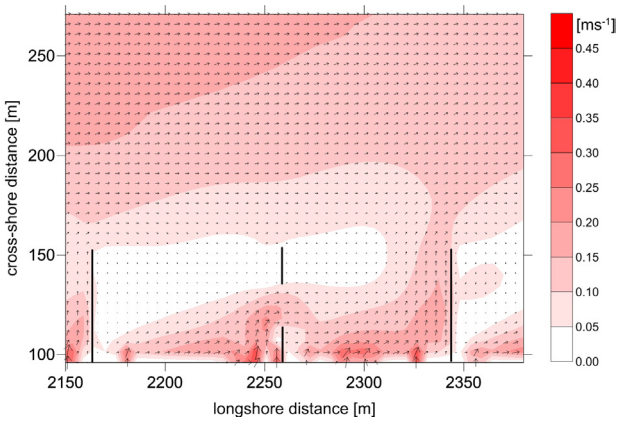

Figure 6

Calculated depth-averaged flow velocities for a groin with a breach about its central part in moderate storm conditions (H_s=1 m, T_p=4 s, α=45°)

Groin with a missing end part (groin shortened by 1/3)

For a groin shorter by 1/3 than the neighboring groins (Fig. 7), the calculated flow velocities are

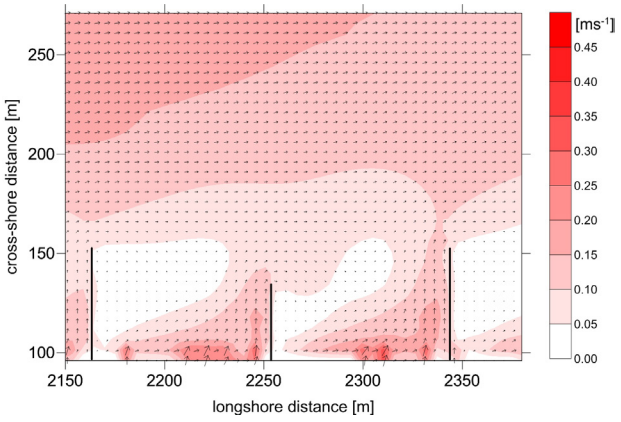

Figure 7

Calculated depth-averaged flow velocities for a groin with missing piles at its end in moderate storm conditions (H_s=1 m, T_p=4 s, α=45°)

similar to those obtained for the groin with a breach in the central part (cf. Fig. 6), while they are smaller in the close vicinity of the shoreline, not exceeding the value of 0.2 m s^{-1}.

The offshore directed current along the shorter groin will move the sediment seaward. In the region of the groin tip, this sediment will be gradually deposited due to the velocity decrease. The intensity of the nearshore erosion will be smaller than in the case of the "central breach" and definitely smaller in comparison to the situation of the "root breach".

Influence of groins on the nourishment duration

It was assumed that the nearshore zone had been subject to artificial nourishment using 30 000 m^3 of sand with the median grain diameter of d_{50}=0.22 mm. The sandy material filled two fields between three neighboring groins (being in good technical condition, without breaches). The computations have yielded parameters of waves and currents in the fields between the groins. The sediment transport rates and the bathymetric changes have also been determined. The sediment transport was modeled using van Rijn's (1993) formulae while the bed shear stresses were calculated with the use of Fredsöe's (1984) integral momentum model. For the sake of comparison, the modeling procedure was also carried out for the same nourished shore but without groins. The coastal bathymetric system was assumed the same in both cases. Three representative sets of wave parameters were taken into consideration:

- mild storm conditions (H_s=1.0 m, T_p=4.0 s, a=45°);
- moderate storm conditions (H_s=1.5 m, T_p=5.0 s, a=45°);
- intensive storm conditions (H_s=2.0 m, T_p=6.0 s, a=45°).

The bathymetric changes were calculated for 24, 48, 72 and 96 hours of storm duration. The volume of sediment washed away from the fields between groins was determined for the following area: 60 m (groin length) × 2 (fields) × 90 m (distance between groins) = 10 800 m^2. Modeling of the sediment transport and nearshore morphodynamics in the respective area (10 800 m^2) was also carried out for the natural shore (without groins). Influence of the groins on the duration of artificial shore nourishment was determined using the coefficient W:

$$W = \left(1 - \frac{V_{groins}}{V_{natural}}\right) \times 100\% \quad (1)$$

where: V_{groins} – nourishment volume washed away from the area covered by 3 groins (2 neighboring fields); $V_{natural}$ – nourishment volume washed away from the respective area of the natural shore.

The results of the computations of the coefficient W (together with approximating curves) are presented in Fig. 8. The value W = 0 means that no supporting role of groins can be expected, while W = 100% denotes the fully effective support of groins. It can be seen in Fig. 8 that the presence of groins results in a larger amount of sandy material placed on the shoreface remains in the nearshore zone compared to the natural shore (without groins). After four days of the continuous wave impact, the amount of washed-out material is reduced by ca. 27-40% due to the supporting role of groins. It is also visible that the positive influence of groins increases for higher (and longer) waves.

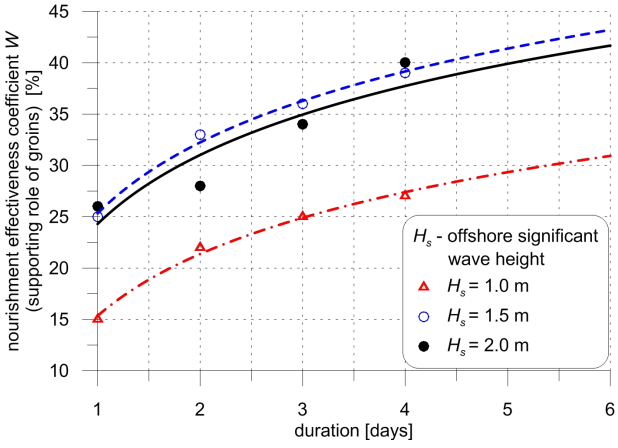

Figure 8

Coefficient W, representing the supporting role of groins in artificial shore nourishment, as a function of time for various offshore wave heights

Submerged breakwaters

General remarks

Submerged breakwaters, being structures located along the shore, induce the wave-breaking process above their crests and trap the sediments tending to move seaward, driven by return currents. These structures are said to work most efficiently

if the predominating waves approach the shore perpendicularly. Compared to the emerged detached breakwaters, the submerged breakwaters generate smaller irregularities of the sea bed and the shoreline. Furthermore, it is believed that they do not cause so strong rip currents and do not affect the landscape values, because they are invisible to tourists and other beach users.

Recent studies concerning the submerged breakwaters or (more generally) low-crested breakwaters proceeded in two directions. Finding cheaper materials to build these structures was the first objective. In this regard, the use of geotextiles was considered (de Groot et al. 2004; Leshchinsky et al. 1996; Koerner et al. 2006). The second group of investigations focused on the description of hydrodynamic effects triggered by this type of structures.

Effectiveness of a structure protecting the shoreline from the retreat largely depends on the transmission of waves over the crest of the structure (Van der Meer & d'Angremond 1991) and its longshore span. There is no perfect theoretical description of the wave transmission over the submerged breakwater crest, which would ensure the optimization of the structure dimensions and the location in the coastal zone, although a lot of work on this topic has been done and published, see e.g. Cappietti (2011). Another still unsolved problem, important to the environment and safety of swimmers, is related to the induction of rip currents in the gaps between segments of submerged breakwaters.

Within the present study, an attempt was undertaken to optimize the dimensions of the segmented submerged breakwaters, like relative water depth at the crest of the structure and its relative length, in order to obtain the maximum wave energy dissipation and the minimum rip current velocities.

Numerical modeling of wave-current fields near submerged breakwaters

The computations of parameters of waves and currents in the presence of submerged breakwaters were carried out using the Delft3D modeling software. The coastal area subject to modeling had the longshore and cross-shore dimensions of 1100 m and 400 m, respectively. This choice was made as a reasonable compromise between the total avoidance of undesirable boundary effects (by moving away from the boundaries) and the reduction of time consumption during the model runs. The computational grid had the 5 m square mesh while the water column was divided using so-called *s* coordinates into 4 layers (39%, 28%, 19% and 14%). A constant sea bottom inclination of 0.02 was assumed to represent a typical south Baltic nearshore area. Three segments of a submerged breakwater were "built" at a distance of 100 m from the shoreline. The height of breakwaters and gaps between them were changed for individual model runs, while the breakwaters' crest width was kept constant in all numerical tests described here, equal to 20 m (4 grid units).

The layout of the submerged breakwaters in the nearshore zone is shown in Fig. 9. Locations of the wave height and flow velocity values included in the present analysis are also given in Fig. 9. The cross-section of the nearshore sea bottom with the submerged breakwater is shown in Fig. 10.

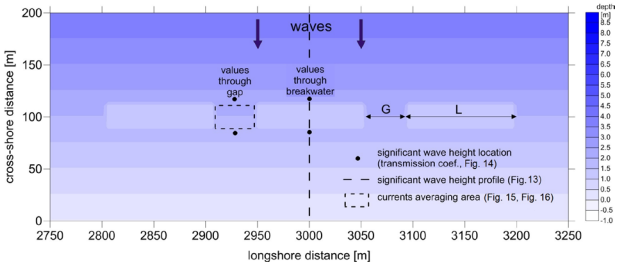

Figure 9

Layout of submerged breakwaters in the nearshore zone (*L* – breakwater segment length, *G* – gap length)

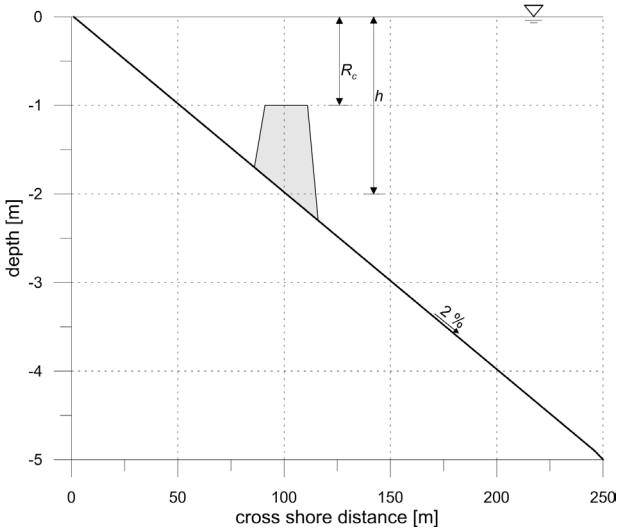

Figure 10

Cross-section of nearshore sea bottom with a submerged breakwater (R_c – water depth at a breakwater crest)

The computations were carried out for waves approaching the shore perpendicularly ($a = 90°$), with the offshore significant wave height $H_s = 2$ m and the wave energy peak period $T_p = 5.5$ s. The model runs comprised the situations with the following ratios of the water depth at the crest to the water depth (R_c/h) and the breakwater segment length to a gap between segments (L/G):

R_c/h	0.20	0.30	0.45	0.50	0.55	0.65	0.80;				
L/G	0.48	0.70	1.00	1.50	2.00	2.63	3.14	3.67	3.83	4.60	4.80.

The typical field of wave height and flow velocity are shown in Figs. 11 and 12, respectively, while wave heights at different distances from the shoreline for $L/G = 0.48$ and $L/G = 4.6$ in the form of curves corresponding to various ratios R_c/h (resulting in various transmission coefficients K_t) are given in Fig. 13. The wave transmission coefficients K_t are also shown in Fig. 13. It should be noted that the values $L/G = 0.48$ and $L/G = 4.6$ represent a very big and very small gap between the breakwater segments, respectively.

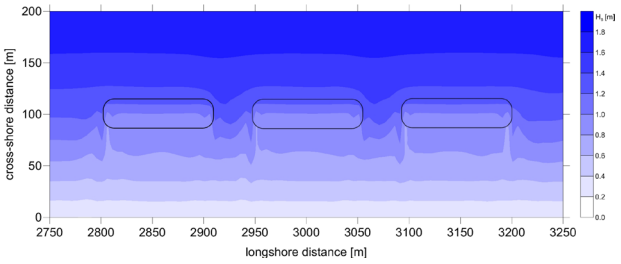

Figure 11

Calculated significant wave heights near submerged breakwaters for R_c/h=0.2 and L/G=2.63 (H_s=2 m, T_p=5.5 s, α=90°)

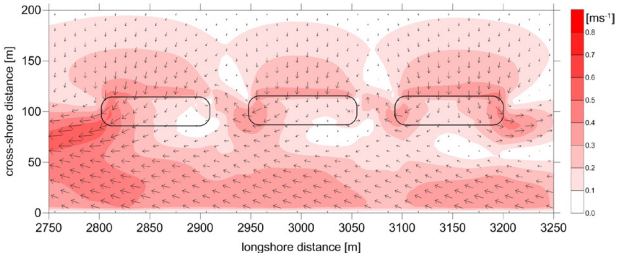

Figure 12

Calculated flow velocities near submerged breakwaters for R_c/h=0.2 and L/G=2.63 (H_s=2 m, T_p=5.5 s, α=90°)

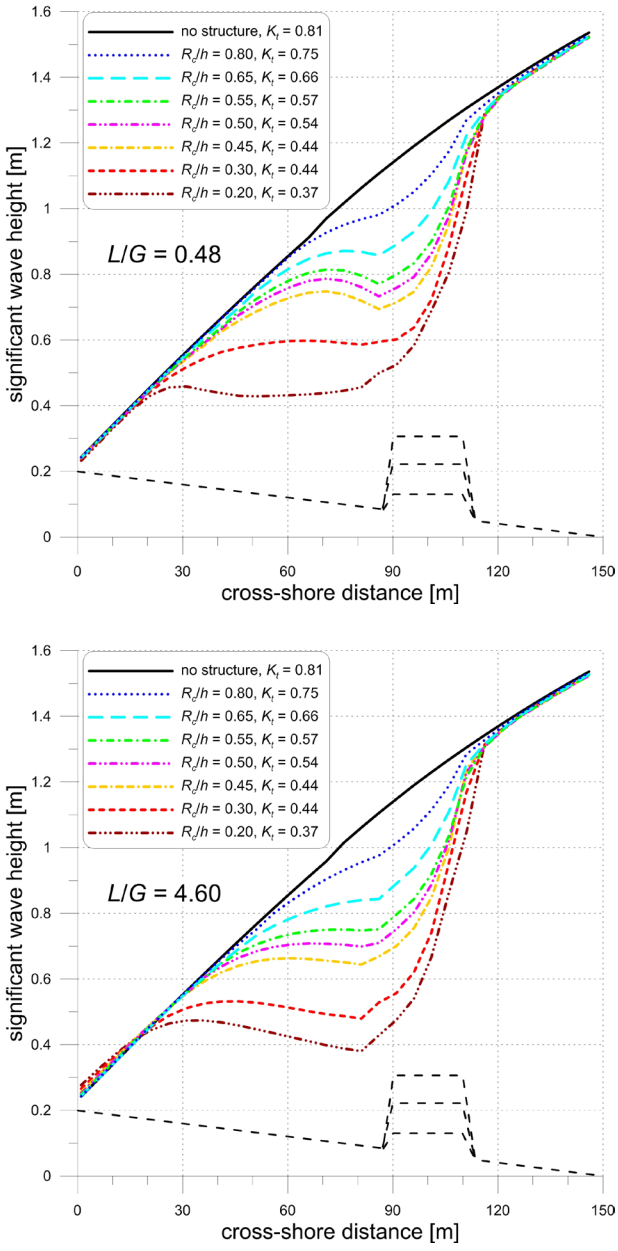

Figure 13

Calculated wave heights at different distances from the shoreline for L/G=0.48 (up) and L/G=4.6 (down) as curves corresponding to various ratios R_c/h resulting in various transmission coefficients K_t (bottom dashed lines indicate location of a breakwater and symbolize variability of its height); H_s=2 m, T_p=5.5 s, α=90°

The results of numerical modeling reveal a clear influence of the relative water depth at the breakwater crest (R_c/h) on the wave transmission coefficient K_t. The values of K_t, however, are very weakly dependent

on the relative length of the breakwater segments (L/G). Slightly smaller transmission coefficients K_t were obtained for long segments (big values of L/G).

The following linear function is obtained through the approximation of the relationship between the wave transmission coefficient K_t and the relative depth at the structure's crest (R_c/h):

$$K_t = a\frac{R_c}{h} + b \qquad (2)$$

Values of the approximating line parameters a and b are given in Table 1, separately for each considered L/G ratio and for the linear approximation comprising all L/G cases. The goodness of fit, as the determination coefficient (R^2), is also presented in Table 1. The approximations of K_t by Eq. (2) are graphically presented in Fig. 14.

At the next stage of the study, the analysis was focused on the assessment of the effect of the gaps between the breakwater segments on the intensity of rip currents generated in these gaps. The considerations presented below make use of the cross-shore velocities averaged over the water depth and over the gap area.

The calculated rip current velocities U_V for various relative depths over the breakwater crest (R_c/h) and various relative breakwater segment lengths (L/G) are shown in Figs. 15 and 16, respectively.

Results of the rip current modeling in the presence of the submerged breakwaters (Figs. 15 and 16) indicate that the respective flow velocities become higher for shorter gaps between the breakwater segments. With the increasing height of the structure (decreasing R_c/h), the rip current velocities initially grow quickly, then reach the maximum and decrease. If the breakwater segments are relatively short (L/G

Table 1

Coefficients (a and b) and goodness (R^2) of linear approximation of the transmission coefficient K_t using the R_c/h ratio for various L/G values and for general approximation

L/G	0.48	0.70	1.00	1.50	2.00	2.63	3.14	3.67	3.83	4.60	4.80	General
A	0.627	0.616	0.644	0.675	0.717	0.712	0.717	0.715	0.704	0.706	0.702	0.686
B	0.253	0.248	0.227	0.205	0.178	0.180	0.171	0.178	0.180	0.183	0.180	0.198
R^2	0.997	1.000	0.997	0.995	0.994	0.995	0.996	0.995	0.997	0.996	0.998	0.987

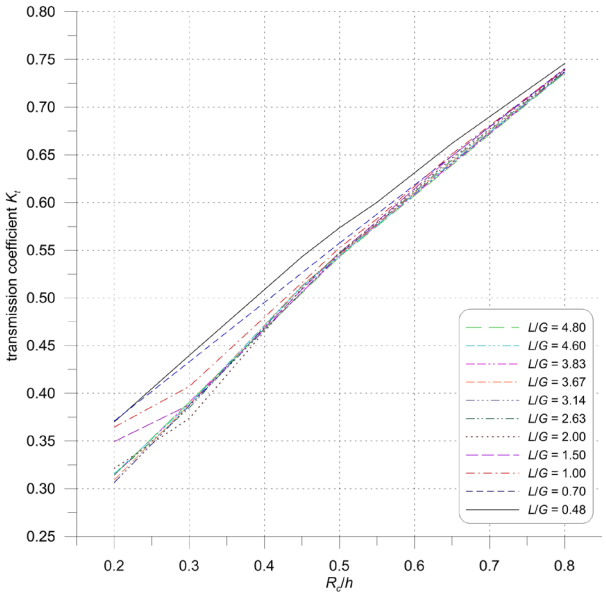

Figure 14

Calculated transmission coefficients K_t as functions of R_c/h for various L/G ratios (H_s=2 m, T_p=5.5 s, α=90°)

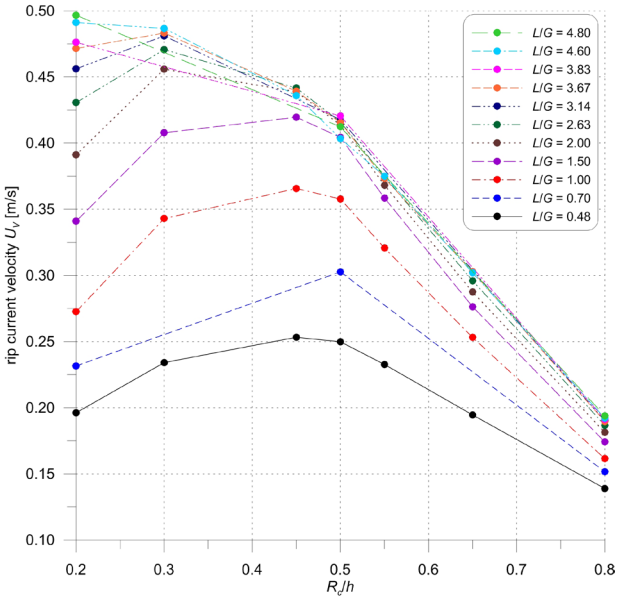

Figure 15

Calculated rip current velocities as functions of R_c/h for various L/G ratios (H_s=2 m, T_p=5.5 s, α=90°)

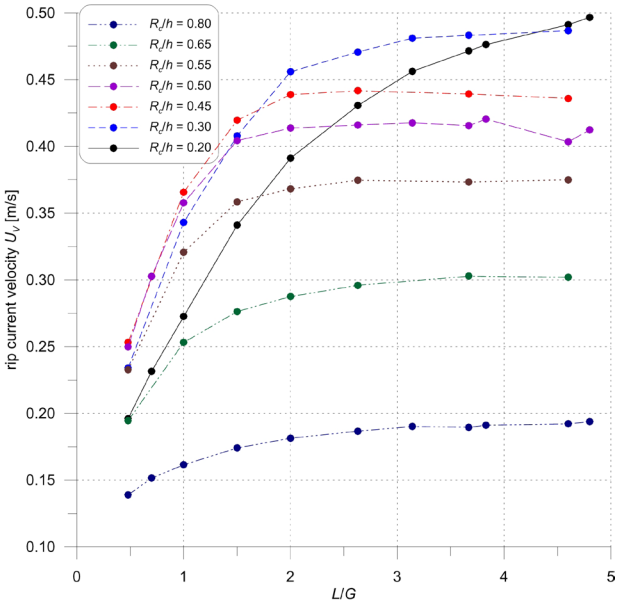

Figure 16

Calculated rip current velocities as functions of *L*/*G* for various R_c/h ratios (H_s=2 m, T_p=5.5 s, α=90°)

= 0.48), the maximum velocity occurs at $R_c/h = 0.45$; for longer segments, this maximum moves toward $R_c/h = 0.2$.

The comprehensive analysis shows that an increase in velocities caused by a decrease in the gap span takes place to the certain *L*/*G* value only. If the relative depth at the structure crest (R_c/h) is greater than 0.5 (which denotes a relatively low breakwater), the rip current velocities do not increase much or do not increase at all for *L*/*G* greater than 2 (structure segments two times longer than gaps). This asymptotic increase in the rip current velocities U_V ("saturation" of the velocities) was approximated by the following function:

$$U_V = A \times \mathrm{tgh}\left(C \times \frac{L}{G}\right) + B \qquad (3)$$

Values of parameters *A*, *B* and *C* of the approximating function given by Eq. (3), together with the goodness of approximations (determination coefficients R^2), are presented in Table 2.

The coefficients *A*, *B* and *C* of the approximating function given by Eq. (3) represent the following features:

A – rate of change (counterpart of the directional coefficient in the linear approximation), the higher *A* the steeper function;
B – intersection of the function with the vertical axis U_V (*B* = 0 for the natural situation, without structures);
C – rate of "saturation" of the approximating curve.

Correlation between the parameters *A*, *B* and *C* and the relative depth at the breakwater crest (R_c/h) is shown in Fig. 17. Analysis of this figure, together with approximations given in Fig. 16, leads to the following findings:

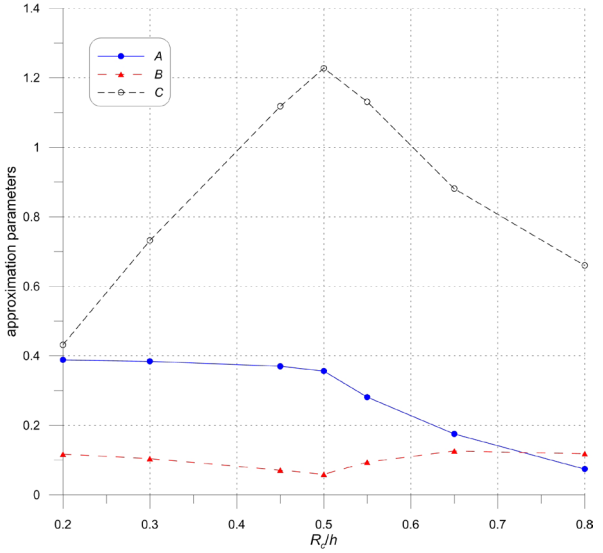

Figure 17

Calculated coefficients *A*, *B* and *C* as functions of R_c/h

Table 2

Coefficients (A, B and C) and goodness (R^2) of approximation (Eq. 3) of rip current velocity U_V using the L/G ratio for various R_c/h quantities

R_c/h	0.20	0.30	0.45	0.50	0.55	0.65	0.80
A	0.388	0.384	0.370	0.356	0.281	0.175	0.074
B	0.117	0.104	0.071	0.059	0.094	0.126	0.118
C	0.432	0.732	1.118	1.228	1.131	0.881	0.660
R^2	1.000	0.999	0.997	0.992	0.999	0.996	0.996

for low structures (R_c/h>0.5)

- functions approximating rip current velocities are less steep;
- for L/G=2 the velocities reach the stage of "saturation", above which their increase is minor;
- the higher breakwaters the bigger the velocities.

for high structures (R_c/h<0.5)

- functions approximating the rip current velocities become steeper;
- the velocity "saturation" point distinctly moves toward longer breakwater segments, which causes higher sensitivity of the rip current velocities to the elongation of segments and suggests that shorter segments should be designed in case a relatively high breakwater is planned.

Discussion and conclusions

Groins

Numerical modeling results show that the flow velocities between groins are much smaller than for the natural shore. For the moderate wave conditions (with the offshore significant wave height of ca. 1 m), these velocities are smaller than the critical values corresponding to the initiation of the bulk sediment transport.

Lack of single piles in the palisade groin does not affect its efficiency, while wider breaches, comprising a few piles, result in the growth of flow velocities through the groin, which consequently causes intensive sea bed erosion at the breaches. Groins with breaches near the shoreline are much more harmful to the shore than the total lack of groins.

Groins in good technical condition increase the effectiveness of the artificial shore nourishment. The computations carried out for the Hel Peninsula show that due to the presence of groins and four days of the continuous wave impact, the amount of material washed away is reduced by at least 27% compared to the natural shore (without groins).

Submerged breakwaters

Transmission of the wave energy over the submerged breakwater is proportional to the relative depth at the breakwater crest (R_c/h).

Relative length of the breakwater segment (L/G) has a small impact on the wave transmission through the structure.

With the increasing height of the structure (decreasing R_c/h), the rip current velocities initially grow quickly, then reach the maximum and decrease. If the breakwater segments are relatively short (L/G = 0.48), the maximum velocity occurs at R_c/h = 0.45, while for longer segments this maximum moves toward R_c/h = 0.2.

It has been found that the correlation between the rip current velocities and the breakwater segment length is different for the structures characterized by R_c/h above and below the value of 0.5. Therefore, the following optimization advice can be followed in the planning of the shore protection with the use of submerged breakwaters:

- for low structures (characterized by R_c/h>0.5), the length of their segments is unimportant for the generation of rip currents, so these segments can be longer to shield the shore in a continuous way on a large longshore span; in this case a moderate reduction in the wave energy is obtained (0.55<K_t<0.75);
- for high structures (characterized by R_c/h<0.5) with the relative length L/G exceeding 2.5 (long segments, narrow gaps), the rip current velocities become dangerously high; in this case, however, a considerable reduction in the wave energy is achieved (0.32<K_t<0.55).

Acknowledgements

We are grateful to the Reviewer for the helpful comments on the previous version of this manuscript. The study was funded by the Ministry of Science and Higher Education, Poland, under the research project N N306 188939 ("Identification, description and parameterization of rip currents in a multi-bar south Baltic coastal zone") and the IBW PAN statutory program No. 2, as well as the research project no. 2012/05/B/ST10/00926 ("Analysis of impact of wind and infragravity waves on coastal and seabed evolution – extension and verification of mathematical and numerical models").

References

Aminti, P., Cammelli, C., Cappietti, L., Jackson, N.L., Nordstrom, K.F., Pranzini, E. (2004). Evaluation of beach response to submerged groin construction at Marina di Ronchi, Italy, using field data and a numerical simulation model. *Journal of Coastal Research*, Special Issue no. 33. Functioning and Design of Coastal Groins: The Interaction of Groins and the Beach-Process and Planning (WINTER 2004), pp. 99-120.

Bacamazo, L. & Grosskopf W. (1999). Beach response to groins. In proceedings of Coastal Sediments, June 21-23 (pp. 2073-2089). New York, USA: ASCE.

Badiei, P., Kamphuis W. & Hamilton D. (1994). Physical experiments on the effect of groins on shore morphology. In proceedings of the 24th International Conference on Coastal Engineering, October 23-28 (pp. 1782-1796). Kobe, Japan: ASCE.

Cappietti, L. (2011). Converting Emergent Breakwaters into Submerged Breakwaters. E Journal of Coastal Research, SI 64 (Proceedings of the 11th International Coastal Symposium), 479-483. Szczecin, Poland, ISSN 0749-0208.

Dabees, M., Moor B. & Humiston K. (2004). Enhancement of T-groins designed to improve downdrift shoreline response. In proceedings of 29th International Conference on Coastal Engineering, September 19-24 (pp. 2423-2435). Lisbon, Portugal: ASCE.

De Groot, M. B., Breteler M.K. & Berendsen E. (2004). Feasibility of geocontainers at the sea shore. In proceedings of 29th International Conference on Coastal Engineering, September 19-24 (pp. 3904-3913). Lisbon, Portugal: ASCE.

Deltares 2010a. Delft3D-WAVE. Simulation of short-crested waves with SWAN – User Manual. Version 3.04, rev. 11114. Deltares, Delft, The Netherlands.

Deltares 2010b. Delft3D-FLOW. Simulation of multi-dimensional hydrodynamic flow and transport phenomena, including sediments – User Manual. Version 3.04, rev. 11114. Deltares, Delft, The Netherlands.

Fleming, C.A. (1990). Principles and Effectiveness of Groynes. In K.W. Pilarczyk (Ed.), Coastal Protection (121-156). Rotterdam, the Netherlands: Balkema Press.

Fredsöe, J. (1984). Turbulent boundary layer in wave-current interaction. *Journal of Hydraulic Engineering ASCE.* 110: 1103-1120.

Hanson, H., Thevenot M. & Kraus C. (1996). Numerical simulation of shoreline change for longshore sand waves at groin field. In proceedings of 25th International Conference on Coastal Engineering, September 2-6 (pp. 4024-4037). Orlando, USA: ASCE.

Hanson, H., Larson M. & Kraus N. (2010). Modelling long-term beach changes under interacting longshore and cross-shore processes. In proceedings of 32th International Conference on Coastal Engineering, 30 June – 5 July (electronic edition). Shanghai, China: Coastal Engineering Research Council.

Koerner, G. & Koerner R. (2006). Geotextile Tube Assessment Using a Hanging Bag Test. *Geotextiles and Geomembranes.* 24: 129-137.

Kunz, H., (1996). Groynes on the East-Frisian Islands: History and experiences. In proceedings of 25th International Conference on Coastal Engineering, September 2-6 (pp. 2128-2141). Orlando, USA: ASCE.

Leshchinsky, D., Leshchinsky O., Ling H.I. & Gilbert P.A. (1996). Geosynthetic tubes for confining pressurized slurry: some design aspects. *Journal of Geotechnical Engineering, ASCE,* 122(8): 682-690.

Nakamura, S. (2010). Passage rate of bedload transport due to a groin in consideration of wave climate. In abstracts of 32th International Conference on Coastal Engineering, 30 June – 5 July (paper 160). Shanghai, China: Coastal Engineering Research Council.

Pilarczyk K. & Zeidler R. (1996). *Offshore breakwater and shore evolution control.* Rotterdam, the Netherlands: A. A. Balkema.

Pruszak, Z., Ostrowski R., Skaja M. & Szmytkiewicz M. (2000). Wave climate and large-scale coastal processes in terms of boundary conditions. *Coastal Engineering Journal,* 42 (1): 31-56.

Pruszak Z. (2004). Polish coast-two cases of human impact. *BALTICA, Vol. 17 (1), 34-40.*

Raudkivi, A. & Dette H. (2002). Reduction of sand demand for shore protection. *Coastal Engineering,* 45: 239-259. DOI: 10.1016/S0378-3839(02)00036-4.

Schoonees, J., Theron A. & Bevis D. (2006). Shoreline accretion and sand transport at groynes inside the port of Richard Bay. *Coastal Engineering,* 53: 1045-1058. DOI: 10.1016/j.coastaleng.2006.06.006.

Schönhofer, J. (2014). Rip currents at beach with multiple bars – theoretical description and *in-situ* observations. PhD thesis, IBW PAN, Gdańsk, 172 pp. (in Polish).

Trampenau, T., Goericke F. & Raudkivi A. (1996). Permeabile pile groins. In proceedings of 25th International Conference on Coastal Engineering, September 2-6 (pp. 2142-2151). Orlando, USA: ASCE.

Uno, Y., Goda Y. & Nobuyuki O. (2010). Suspended-sediment-based beach morphology model applied to submerged groin system. In proceedings of 32th International Conference on Coastal Engineering, 30 June – 5 July (electronic edition). Shanghai, China: Coastal Engineering Research Council.

Van der Meer, J.W. & d'Angremond K. (1991). Wave transmission

at low crested structures. In the proceedings of Conference Coastal Structures and Breakwaters. November 6-8 (pp. 25-42). London, England: ICE & Held.

Van Rijn, L.C. (1993). *Principles of sediment transport in rivers, estuaries and coastal seas*. The Netherlands: Aqua Publications.